Planetary Obliquities with the NASA Roman Coronagraph

Type of observation:

☐ Technology Demonstration☒ Scientific Exploration

Scientific / Technical Keywords: companion (exoplanet), companion (substellar), self-luminous

Required Detection Limit:

$\geq 10^{-5}$	10^{-6}	10^{-7}	10^{-8}	10^{-9}
X	X	X	X	X

Roman Coronagraph Observing Mode(s):

roman coronagraph observing mode(s)							
Band	Mode	Mask Type	Coverage	Support			
1, 575 nm	Narrow FoV	Hybrid Lyot	360°	Required (Imaging),			
	Imaging			Best Effort (Polarimetry)			
1, 575 nm	Wide FoV	Shaped Pupil	360°	Best Effort			
	Imaging			(Imaging and polarimetry)			
4, 825 nm	Wide FoV	Shaped Pupil	360°	Best Effort			
	Imaging			(Imaging and polarimetry)			

Summary: Planetary obliquities provide foundational insights into the early evolution of exoplanet systems, including their formation channels and the prevalence of giant impact phases, secular tilting mechanisms, and other avenues toward obliquity excitation. However, only a handful of exo-planetary obliquity measurements have been obtained to date, due, in large part, to the inherent challenge of characterizing photometric variability at extreme contrast ratios. Roman coronagraphy has the potential to, for the first time, build a sample of exoplanets with precisely measured *planetary* obliquities through continuous monitoring of photometric variability – simultaneously delivering key insights into planetary rotation rates and atmospheric structure. Roman can also measure the configurations of analog systems with companion brown dwarfs and stars, offering empirical constraints on the distinct formation mechanisms of substellar and stellar companions.

Table of Example Targets: Our science case applies to bright directly imaged (self-luminous) planets, as well brown dwarfs and stars at comparable orbital separations, for which Roman will be sensitive to rotational modulation through timeseries observations. Here we list a non-exhaustive sample of targets for this science case, focusing on challenging planet and brown dwarf targets that would most benefit from Roman's precision. For all listed targets, $v \sin i_p$ has already been measured or is projected to be measurable using high-resolution spectrographs on ground-based telescopes [e.g. 1, 2], and orbital inclination has already been constrained through a measured astrometric orbit [e.g. 3, 4, 5, 6, 7]. To derive the companion obliquity for each target, we propose to measure rotation periods $P_{\rm rot}$ by observing photometric variability with Roman.

We provide detection limits under the assumption that, to reliably measure photometric variability in a given source, we must be able to detect variability at the 5% level, requiring sensitivity a factor of 20 better than the projected star-planet contrast. We consider the projected separation at an arbitrarily chosen date of December 1st, 2027. Contrast estimates are made for Band 4, assuming iron/silicate clouds and planet radii $R_p = 1R_{\rm Jup}$.

Name	host star	detection	separation (")	description of target
	V mag.	limit	(or extent)	
HR 8799	5.9	5×10^{-8}	0.96''	c planet
HR 8799	5.9	5×10^{-8}	0.70"	d planet
κ And	4.1	5×10^{-8}	0.62''	b planet / brown dwarf
PZ Tel	8.3	3×10^{-5}	0.74''	b brown dwarf
HIP 64892	6.8	1×10^{-6}	1.31"	b brown dwarf
HD 202772A	8.3	1×10^{-2}	1.3"	B star

Optional Questions:

Are any example targets binary systems in the Washington Double Star survey or other binary survey? N/A

Do any of your example Hybrid Lyot coronagraphic target stars have angular diameters > 2~mas?~N/A

Anticipated Technology / Science Objectives:

Our primary science objective is to characterize the distribution of planetary obliquities – the relative angle between the planet's spin axis and its orbital angular momentum vector – in extrasolar systems. For wide-orbiting ($a \gtrsim 5$ au) planets probed through direct imaging, planetary obliquities may be excited out of alignment with the natal protoplanetary disk's angular momentum through giant impacts [8], asymmetric infall during molecular cloud collapse [9], or spin-orbit resonances [e.g. 10, 11, 12]. Each of these mechanisms may produce a broad range of axial tilts, such that large planetary obliquities are expected to be common, as is seen in the solar system. Yet, this hypothesis has not been directly tested.

Only 4 obliquities have been published for planetary-mass objects, all of which are at the extremes of mass (\sim 10-20 M_J) and separation (\sim 100s of AU) [13, 14, 15, 16]. These four obliquities are each consistent with misalignment through turbulent top-down formation. However, the existing sample does not probe lower planetary masses, for which other lines of evidence, such as the orbital eccentricity distribution, are suggestive of a distinct, bottom-up formation pathway [17]. Roman will, for the first time, offer the capability to probe the obliquities of lowermass ($\lesssim 10 M_J$) directly imaged exoplanets, which may be shaped by a fundamentally distinct set of physical processes. Furthermore, Roman's optical/infrared wavelength coverage complements JWST's near-infrared observations, providing constraints on the vertical properties of heterogeneous atmospheric structures even for targets with previously reported photometric variability signatures [e.g. 18, 19].

As a corollary, we also suggest that planetary obliquities may be contextualized through a direct comparison with brown dwarf and stellar companion analog systems at comparable orbital separations to directly imaged planets. These observations will add a new dynamical probe to shape the empirical boundary between planet, brown dwarf, and star formation regimes.

Alongside obliquities, our proposed observations will provide measurements of planet, brown dwarf, and stellar spin rates, which are derived using the same time-series photometric observations required for our primary science case. These spin rates may shed light on the spin-down of planetary systems over time [e.g. 2] – particularly when comparing the population of young, self-luminous planets with any older planets that Roman is projected to detect in the optical. A joint comparison of the obliquities, spin rates, and orbital eccentricities of planets, brown dwarfs, and stars will provide a uniquely comprehensive dynamical grounding to parse the distinct evolutionary processes shaping each class of objects.

Is this observation appropriate for "first-look" / commissioning (<3 months after launch), the observation phase (< 18 months after "first-look" / commissioning), or a potential extended observing phase?:

We require sufficient sensitivity to observe planetary variability at the 5% level, such that the core of our science case requires the improved contrast of Band 4 (by comparison with Band 1, in which our targets are substantially fainter). Most or all of our planetary-mass targets will likely not be appropriate for the commissioning phase as a result, and they would instead require observations in the later stages of the mission, when improved detection limits have been achieved.

However, some targets from a comparison sample of relatively low-contrast brown dwarf and stellar companions to analog host stars, which will be useful to contextualize our proposed planetary obliquity measurements, may be well-suited for and scientifically valuable to study during the commissioning phase. Because obliquity is a geometric property of the systems, a comparison from results derived across different wavelength bands – that is, comparing stellar/brown dwarf obliquities drawn from Band 1 to planetary/brown dwarf obliquities drawn from Band 4 – would still be valuable.

Observing Description: We propose to build a census of planetary obliquity measurements by combining time-series photometry observations from the NASA Roman mission with ground-based rotational line broadening constraints from near-infrared high-resolution spectroscopy, as well as astrometric orbit arcs. Photometry provides a rotation period $P_{\rm rot}$ that, in combination with planetary radius R_p — which can be derived from planetary flux under the assumption of blackbody radiation — enables calculation of the equatorial rotational velocity $v_{\rm eq} = (2\pi R_p)/P_{\rm rot}$. Ground-based high-resolution spectroscopy of the isolated flux from each planet provides a constraint on projected planetary rotation $v \sin i_p$, which can be used to determine the planetary inclination i_p via the relation $i_p = \arcsin{(\frac{v \sin i_p}{v_{\rm eq}})^1}$. The planet's orbital inclination $i_{\rm orb}$ can be derived via astrometric measurements that trace the orbital arc of the planet. A comparison of i_p and $i_{\rm orb}$ yields a constraint on the planetary obliquity ψ_p .

Our primary observable with Roman is photometric variability of directly imaged planets. This requires continuous observations over the course of one or more planetary rotation periods. Previous work has shown that planetary-mass companions typically spin at $\approx 10\%$ of their breakup rotation rate, corresponding to $P_{\rm rot} \approx 5-25$ hours [2]. For comparison, Jupiter and Saturn have rotation rates $P_{\rm rot} \approx 10-11$ hours, while Neptune and Uranus have $P_{\rm rot} \approx 16-17$ hours.²

We conservatively estimate, therefore, that each planet will require 25 hours of continuous photometric observations to trace one or more full rotational periods. Reconnaissance observations of 3-5 hours may be used to vet each target for projected rotation period and photometric amplitude. Brown dwarf rotation periods range up to a few days, and stellar rotation periods up to tens of days; due to their higher-amplitude signals, many of these targets would not require continuous monitoring. Stellar binaries also do not require the coronagraph or reference stars.

The highest-amplitude photometric variability detection to date for a planetary-mass object is 24.7% for VHS 1256-1257ABb at 1.27 μ m [18], or 5.76% at 4.5 μ m [19]. Past searches have also placed upper limits on variability for other directly imaged planets, such as HR 8799 b (5-10%), c (10%), and d (30%) [21, 22, 23]. We assume that, to reliably measure a source's obliquity, we must be able to detect variability at the 5% level. Depending on the system orientation, we note that precision down to 0.5-1% may be required for some targets [24].

¹Correlated uncertainties in these measurements may be accounted for using the framework of [20].

 $^{^2}$ The solar system rocky planets rotate much more slowly: Venus's rotation period is $P_{\rm rot} \approx 243$ days. However, the giant planets probed by direct imaging are expected to spin closer at rates closer to breakup due to runaway accretion and conservation of angular momentum.

Estimate of Time Needed:

Photometric variability constraints require multiple observations over the course of the object's spin period, such that temporal flux changes are resolvable. Ideally, therefore, targets should require integration times no more than roughly 1/5 the predicted rotation period of the object. This corresponds to roughly 1 hour for the fastest-spinning planets, or 5 hours for slower-rotating planets. Longer integration times are acceptable, but in many cases will not be required (due to the lower contrast of the systems), for brown dwarfs and stars, which spin more slowly.

We used the Roman Corgi-ETC³ to predict the exposure times necessary to reach SNR 5 in Band 4 for each of our targets. More specifically, we consider the exposure times required to reach SNR 5 at the contrast levels needed to detect 5% variability for each of our example targets. We find that our most challenging listed targets (HR 8799 c and d) require up to 1.1/1.6 hours of integration time to reach SNR 5 in the optimistic/conservative case, while a 1-hour observation can reach SNR 55 for our lowest-contrast listed brown dwarf, PZ Tel, even in the conservative case. In total, time-resolved observations tracking 1-2 rotation periods would take an estimated 25 hours of continuous integration time per planet or low-mass brown dwarf. Slower-spinning stars and high-mass brown dwarfs with high-amplitude rotation signals may be more sparsely sampled – for example, with 3-5 visits of a few hours each over the course of the target's projected rotation period.

³https://github.com/roman-corgi/corgietc

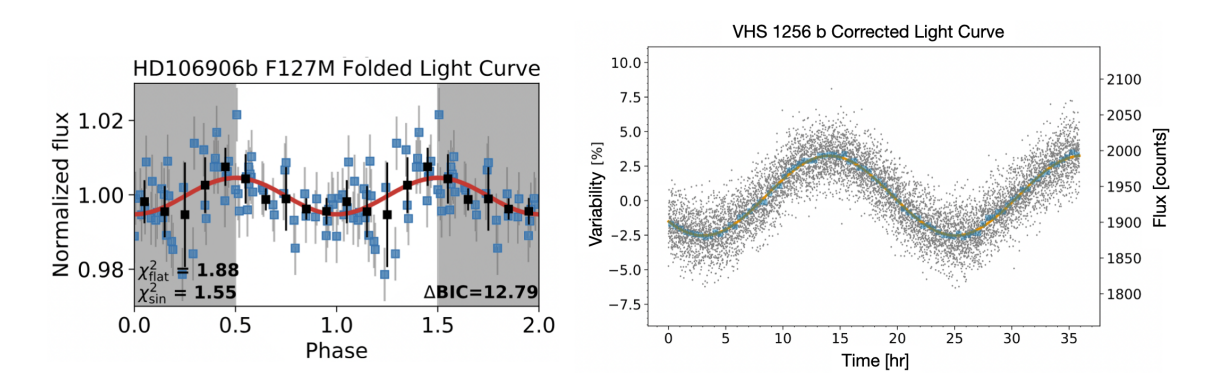


Figure 1: Left: Hubble F127M photometry of HD 106906 b, showing sinusoidal variability with an amplitude of 0.5%. Right: Spitzer 1-5 μ m light curve of VHS 1256 b, showing sinusoidal variability with an amplitude of 5.76%. Figure adapted from [25] and [19].

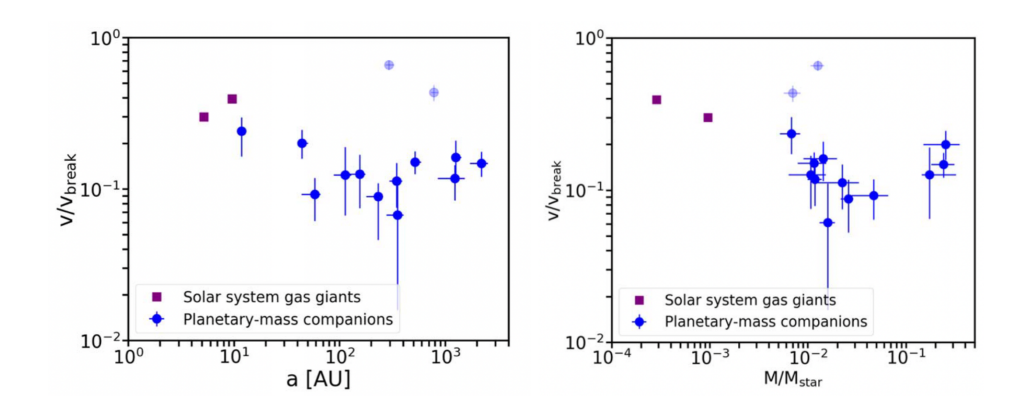


Figure 2: Rotational velocities of solar system and directly imaged gas giants, scaled by the planetary breakup velocity $v_{\rm break}$. No significant dependence between rotation rate and either semimajor axis (left panel) or mass ratio (right panel) has been observed to date, such that projected rotational velocities may be predicted primarily through $v/v_{\rm break}$. Figure adapted from [2].

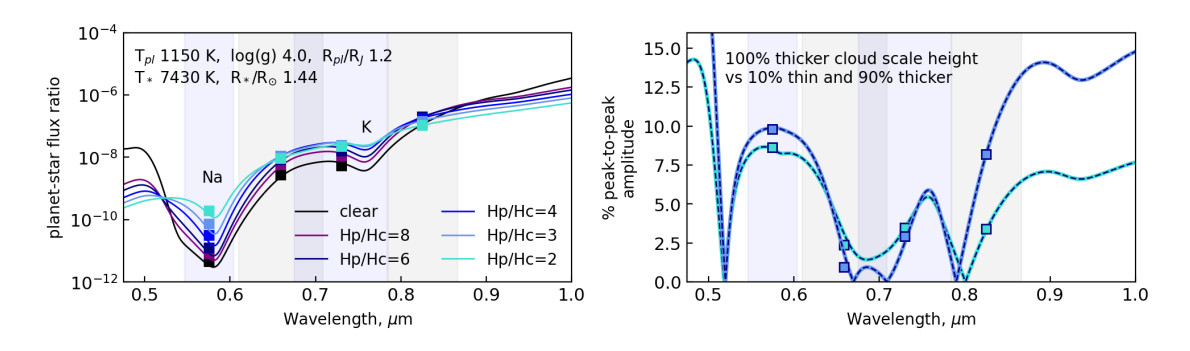


Figure 3: Projected variability across the Roman-CGI bandpasses for \sim HR 8799 d or c, under the assumption that variability arises from a 10% change in the fractional area with a vertically thin cloud layer.

References

- [1] Ignas A. G. Snellen et al. "Fast spin of the young extrasolar planet β Pictoris b". In: 509.7498 (May 2014), pp. 63–65. DOI: 10.1038/nature13253.
- [2] Marta L. Bryan et al. "As the Worlds Turn: Constraining Spin Evolution in the Planetarymass Regime". In: 905.1, 37 (Dec. 2020), p. 37. DOI: 10.3847/1538-4357/abc0ef. arXiv: 2010.07315 [astro-ph.EP].
- [3] A. Zurlo et al. "Orbital and dynamical analysis of the system around HR 8799. New astrometric epochs from VLT/SPHERE and LBT/LUCI". In: 666, A133 (Oct. 2022), A133. DOI: 10.1051/0004-6361/202243862. arXiv: 2207.10684 [astro-ph.EP].
- [4] Sarah Blunt et al. "First VLTI/GRAVITY Observations of HIP 65426 b: Evidence for a Low or Moderate Orbital Eccentricity". In: 166.6, 257 (Dec. 2023), p. 257. DOI: 10.3847/1538-3881/ad06b7. arXiv: 2310.00148 [astro-ph.EP].
- [5] C. Desgrange et al. "In-depth direct imaging and spectroscopic characterization of the young Solar System analog HD 95086". In: 664, A139 (Aug. 2022), A139. DOI: 10.1051/0004-6361/202243097. arXiv: 2206.00425 [astro-ph.EP].
- [6] Taichi Uyama et al. "Atmospheric Characterization and Further Orbital Modeling of κ Andromeda b". In: 159.2, 40 (Feb. 2020), p. 40. DOI: 10.3847/1538-3881/ab5afa. arXiv: 1911.09758 [astro-ph.EP].
- [7] Kathryn V. Lester et al. "Visual Orbits and Alignments of Planet-hosting Binary Systems". In: 166.4, 166 (Oct. 2023), p. 166. DOI: 10.3847/1538-3881/acf563. arXiv: 2308. 16826 [astro-ph.SR].
- [8] V. S. Safronov. "Sizes of the largest bodies falling onto the planets during their formation". In: 9 (June 1966), pp. 987–991.
- [9] S. Tremaine. "On the origin of the obliquities of the outer planets". In: 89.1 (Jan. 1991), pp. 85–92. DOI: 10.1016/0019-1035 (91) 90089-C.
- [10] Douglas P. Hamilton and William R. Ward. "Tilting Saturn. II. Numerical Model". In: 128.5 (Nov. 2004), pp. 2510–2517. DOI: 10.1086/424534.
- [11] William R. Ward and Douglas P. Hamilton. "Tilting Saturn. I. Analytic Model". In: 128.5 (Nov. 2004), pp. 2501–2509. DOI: 10.1086/424533.
- [12] Sarah Millholland and Konstantin Batygin. "Excitation of Planetary Obliquities through Planet-Disk Interactions". In: 876.2, 119 (May 2019), p. 119. DOI: 10.3847/1538-4357/ab19be. arXiv: 1904.07338 [astro-ph.EP].
- [13] Marta L. Bryan et al. "Obliquity Constraints on an Extrasolar Planetary-mass Companion". In: 159.4, 181 (Apr. 2020), p. 181. DOI: 10.3847/1538-3881/ab76c6. arXiv: 2002. 11131 [astro-ph.EP].
- [14] Marta L. Bryan et al. "Obliquity Constraints on the Planetary-mass Companion HD 106906 b". In: 162.5, 217 (Nov. 2021), p. 217. DOI: 10.3847/1538-3881/aclbb1. arXiv: 2108.13437 [astro-ph.EP].

- P. Palma-Bifani et al. "Peering into the young planetary system AB Pic. Atmosphere, orbit, obliquity, and second planetary candidate". In: 670, A90 (Feb. 2023), A90. DOI: 10.1051/0004-6361/202244294. arXiv: 2211.01474 [astro-ph.EP].
- [16] Michael Poon et al. "Leaning Sideways: VHS 1256-1257 b is a Super-Jupiter with a Uranus-like Obliquity". In: 168.6, 270 (Dec. 2024), p. 270. DOI: 10.3847/1538-3881/ad84e5.arXiv: 2410.02672 [astro-ph.EP].
- [17] Brendan P. Bowler, Sarah C. Blunt, and Eric L. Nielsen. "Population-level Eccentricity Distributions of Imaged Exoplanets and Brown Dwarf Companions: Dynamical Evidence for Distinct Formation Channels". In: 159.2, 63 (Feb. 2020), p. 63. DOI: 10.3847/1538-3881/ab5b11. arXiv: 1911.10569 [astro-ph.EP].
- [18] Brendan P. Bowler et al. "Strong Near-infrared Spectral Variability of the Young Cloudy L Dwarf Companion VHS J1256-1257 b". In: 893.2, L30 (Apr. 2020), p. L30. DOI: 10. 3847/2041-8213/ab8197. arXiv: 2004.05170 [astro-ph.EP].
- [19] Yifan Zhou et al. "Spectral Variability of VHS J1256-1257b from 1 to 5 μ m". In: 160.2, 77 (Aug. 2020), p. 77. DOI: 10.3847/1538-3881/ab9e04. arXiv: 2004.05168 [astro-ph.EP].
- [20] Kento Masuda and Joshua N. Winn. "On the Inference of a Star's Inclination Angle from its Rotation Velocity and Projected Rotation Velocity". In: 159.3, 81 (Mar. 2020), p. 81. DOI: 10.3847/1538-3881/ab65be. arXiv: 2001.04973 [astro-ph.IM].
- Dániel Apai et al. "High-cadence, High-contrast Imaging for Exoplanet Mapping: Observations of the HR 8799 Planets with VLT/SPHERE Satellite-spot-corrected Relative Photometry". In: 820.1, 40 (Mar. 2016), p. 40. DOI: 10.3847/0004-637X/820/1/40. arXiv: 1602.02856 [astro-ph.EP].
- [22] Beth A. Biller et al. "A high-contrast search for variability in HR 8799bc with VLT-SPHERE". In: 503.1 (May 2021), pp. 743-767. DOI: 10.1093/mnras/stab202. arXiv: 2101. 08514 [astro-ph.EP].
- [23] Jason J. Wang et al. "Atmospheric Monitoring and Precise Spectroscopy of the HR 8799 Planets with SCExAO/CHARIS". In: 164.4, 143 (Oct. 2022), p. 143. DOI: 10.3847/1538-3881/ac8984. arXiv: 2208.05594 [astro-ph.EP].
- [24] Xianyu Tan and Adam P. Showman. "Atmospheric circulation of brown dwarfs and directly imaged exoplanets driven by cloud radiative feedback: effects of rotation". In: 502.1 (Mar. 2021), pp. 678–699. DOI: 10.1093/mnras/stab060. arXiv: 2005.12152 [astro-ph.EP].
- Yifan Zhou et al. "Cloud Atlas: High-precision HST/WFC3/IR Time-resolved Observations of Directly Imaged Exoplanet HD 106906b". In: 159.4, 140 (Apr. 2020), p. 140. DOI: 10. 3847/1538-3881/ab6f65. arXiv: 2001.08304 [astro-ph.EP].